Phaeodactylum tricornutum as a source of value-added products: A review on recent developments in cultivation and extraction technologies

Phaeodactylum tricornutum as a source of value-added products: A review on recent developments in cultivation and extraction technologies

Caterina Celi[1], Debora Fino[1,2*], Francesco Savorani[1]

[1]Department of Applied Science and Technology, Politecnico di Torino, Turin, Piemonte, 10129, Italy

[2] Istituto Italiano di Tecnologia, Center for Sustainable Future Technologies, Turin, Piemonte, 10144, Italy

[*]Corresponding author: Debora Fino, e-mail: debora.fino@polito.it, Politecnico di Torino, Turin, Piemonte, 10129, Italy

Abstract

Microalgae are photosynthesizing organisms that produce high-value metabolites by using CO_2 as a feedstock, potentially promoting sustainable manufacturing solutions. They are indeed rich in polyunsaturated fatty acids, pigments, polysaccharides, and proteins, which are widely employed in the pharmaceutical, nutraceutical, cosmetic, and food sectors. Among marine diatoms, *Phaeodactylum tricornutum* is one of the most studied species and commercially suitable strain for large-scale cultivation thanks to its capacity to accumulate commercially relevant metabolites such as EPA, chrysolaminarin, and fucoxanthin. It can successfully operate phototrophy, but mixotrophy mode was revealed to enhance the growth rate and biomass concentration and quality. This review collects recent findings in cultivation strategies and extraction technologies tested on this species so far. The culture performances are discussed and a comparison between mixotrophic and phototrophic conditions is provided. Finally,

successful biorefinery extraction cascades experimented on this diatom are described to foster research in this direction.

Keywords: *Phaeodactylum tricornutum*; algal cultivation; extraction technologies; value-added products; biorefinery concept

1. Introduction

The climate change consequences that we are forced to face nowadays demand urgent change in society, especially in the manufacturing and transport sectors. There is a need to replace petroleum-based commodities and fuels with biobased ones before the consequence of industrialization will become overwhelming for our planet.

Recent political strategies have been implemented to facilitate the transition to a circular bioeconomy model, able of ensuring both economic growth and preservation of natural resources. Hope and effort in this sense have been placed on microalgae, key players in blue biotechnology because they can offer a significant contribution to the building of this sustainable economy model by providing both low-value and high-volume products, and high-value and low-volume products.

Beyond the several microalgae strains that are currently studied at a research level, industrial-scale cultivations have also arisen to exploit the intrinsic capacity of some strains to accumulate specific metabolites, like ß-carotene from *Dunaliella salina* or astaxanthin from *Haematococcus pluvialis,* not to mention the long-established use of algae as a food ingredient in the Asiatic continent.

The present review proposes a literature collection on *Phaeodactylum tricornutum*, a model diatom, which has been already examined at a laboratory scale and whose industrial potential has been revealed. The ultimate scope is to provide the optimal cultivations conditions that have arisen from numerous studies conducted through the

50 years and how these influence the final biochemical composition and its consequent
51 applicability.

52 **1.1 Diatoms overview**

53 Diatoms are single-celled algae belonging to the group of eukaryotic phytoplankton that
54 have existed for more than 180 million years. Present in many areas of the world, they
55 are particularly widespread at high latitudes and in coastal ecosystems rich in nutrients
56 (Malviya et al., 2016). They can have radial symmetry, in the case of centric diatoms, or
57 bilateral symmetry as for pennate diatoms. These unicellular photosynthetic organisms,
58 sizing from 1 μm to 200 μm, undertake significant roles in the major biogeochemical
59 cycles, such as carbon sequestration, oxygen production, and nutrient recycling,
60 especially nitrogen, carbon, and silicon. About 20% of global carbon fixation can be
61 indeed ascribed to diatoms (Hockin et al., 2012) which produce, through their
62 photosynthetic apparatus, more than 20% of the world's oxygen production.
63 Furthermore, they provide a large amount of organic matter, about 25% of global
64 biomass production, thus supplying nourishment to most other aquatic organisms (Not
65 et al., 2012).
66 Given their global distribution, diatoms present high variability and diversification.
67 Researchers often attempted to estimate the numbers of diatom species through time:
68 the latest values are from 1800 planktonic species to 200000, more than any other single
69 algal class. Because of their complex evolutionary history and genomic reorganization,
70 diatoms have developed a range of potentially useful features, such as a rigid silicified
71 cell wall called frustule, vacuoles for nutrient storage, fast reactions to changes in
72 environmental conditions, resting stage formation, ice-binding proteins, and a urea cycle
73 (Malviya et al., 2016).

The frustules are constituted of silicic acid and other organic materials, whose morphology may vary according to environmental factors and cell condition. The presence of silica in diatoms has also been related to the formation of diatomite, which has been commercially mined for many uses. Indeed, along geological periods, diatoms' death and decomposition entail the formation of sediments of silicon on the seafloor, which constitutes this diatomaceous earth or diatomite (Branco-Vieira et al., 2018). Other valuable and interesting metabolites can be found in diatom chloroplasts, such as chlorophyll *a, c1,* and *c2,* and a complement of accessory pigments, including xanthophylls and carotenes. The light-harvesting pigments chlorophyll a, chlorophyll c, and fucoxanthin together constitute the complex fucoxanthin-chlorophyll protein (FCP), which has the function of harvesting the light necessary for diatoms. The pigment fucoxanthin is also responsible for the golden-brown color of these microalgae, being the most abundant pigment. Nowadays, seaweeds represent the main source of fucoxanthin at industrial scale. Nevertheless, marine diatoms accumulate 5-10 fold higher amounts (2.24 to 26.6 mg g^{-1} DW) and thereby are regarded as a potential source of this valuable pigment (Pereira et al., 2021).

Carotenoids instead are involved in cell photoprotection when the variability in light intensity, typical of the marine ecosystem, threatens to assimilate overmuch light energy and, consequently, may compromise photosynthetic productivity through a mechanism called photoinhibition. This process, occurring when light energy is absorbed beyond the photosynthetic capacity of the cell, involves the production of reactive oxygen species (ROS) like hydroxyl radicals (OH•), superoxide anions (O_2^-), hydrogen peroxide (H_2O_2), and singlet oxygen ($^1O_2$), that can provoke the oxidization of any pigment, lipid, or protein nearby, thus damaging the photosynthetic apparatus (Jallet et

al., 2016). To prevent photoinhibition diatom cells have developed an assortment of defence tools, such as the diadinoxanthin cycle associated with diadinoxanthin de-epoxidation and diatoxanthin epoxidation. The latter is indeed directly involved in the dissipation of energy through the action of Non-Photochemical Quenching (NPQ), which allows the photoacclimation of the light-harvesting system (Kooistra et al., 2007). The presence of diadinoxanthin, diatoxanthin, and additionally violaxanthin, antheraxanthin, and zeaxanthin can be noted especially in cells subjected to excessive light energy (Kuczynska et al., 2020).

Lipids and carbohydrates instead represent energy storage metabolites. In particular, carbohydrates can be sorted into insoluble and soluble. The first ones are structural carbohydrates that are frustule-associated sugars, such as sulphated glucoromannans, callose, and chitin; whereas, soluble carbohydrates are chrysolaminarin, exopolysaccharides or extracellular polysaccharides (EPS), and free sugars (Caballero et al., 2016). Among polysaccharides, chrysolaminarin constitutes the preferred energy storage for diatoms and normally accounts for 10-20% of the total carbon in cells at the exponential stage (Kroth et al., 2008). It is constituted of a backbone of β-1,3-D-glucose units linked together, with a degree of branching of 0-0.2 at position 6 and a degree of polymerization of 5-60. Its accumulation occurs in vacuoles inside the cell during the photosynthetically active light periods, while it is consumed in the dark to fuel heterotrophic metabolism (Caballero et al., 2016).

Regarding the lipidic fraction, different types of lipids can be detected in these microalgae: fatty acids, polar lipids, non-polar lipids, triacylglycerides (TAGs), steroids, and oxylipins. Diatoms' cell membrane is predominantly composed of fatty acids, which comprise between 15 and 25% of their biomass. Common in diatoms are the

saturated fatty acid myristic acid (C14:0) and palmitoleic acid (C16:1), belonging to monounsaturated fatty acids (MUFAs). Polyunsaturated fatty acids (PUFAs) are instead composed of 18-22 carbon chains with two or more double bonds. Stearidonic acid (SDA, 18:4), α-linolenic acid (ALA, 18:3), eicosapentaenoic acid (EPA, 20:5) and docosahexaenoic acid (DHA, 22:6) belong to ω -3 PUFAs group; while ω-6 PUFAs are for example arachidonic acid (ARA, 20:4) and γ-linoleic acid (GLA, 18:3). PUFAs, particularly the ω-3 category, have gained great visibility through the years thanks to their role as bioactive substances and as essential nutrients promoting human health. The relative amounts of storage carbon that accumulate in lipids and carbohydrates can be modified by altering the cell's physiological condition as a result of the breakdown of some biosynthetic pathways and the activation of new ones, involving increased production of lipids or carbohydrates. For example, nitrogen depletion has been a widely tested strategy to manipulate algal metabolism with the intent of favoring lipids production. It was also argued that a boosted production of TAG can be stimulated by blocking the polysaccharides metabolism through genetic engineering, as the resulted unplaced storage carbon would be relocated to other storage metabolites, in this case, lipids. (Caballero et al., 2016).

Hence, it is evident how diatoms can be a potential feedstock for numerous biotechnological purposes and an extensive line of applications in industry. Besides their interesting biochemical composition and ability to produce valuable metabolites, they exhibit a high capacity to thrive in both fresh and marine water and do not require fertile lands, if compared to biomass produced by terrestrial crops. Moreover, they rapidly adapt to changing nutrient conditions and provide high biomass production rates. Despite these advantages, their commercialization and industrialization still lack

146 to be standardized at a large scale, mainly due to regulatory and technological barriers,
147 such as the high water, energy, and nutrients consumption during the cultivation step
148 and some technical hindrances to biomass recovery. Currently, the industrial production
149 of microalgae for commercial purposes is related to a cost of 3.4 € kg^{-1} for a
150 hypothetical Spanish production plant (Penhaul Smith et al., 2020). However,
151 production costs are subjected to variations depending on different factors, including the
152 cultivation system (photobioreactors or open ponds), costs associated with workforce,
153 operating costs, etc. Therefore, the gaps in the realization of large-scale cultivation,
154 such as plant capability and dimension, and standardization of cultivation methods must
155 be filled. The limits in the commercialization of high-value products need to be
156 overcome by testing cheap and sustainable extraction technologies. Moreover, further
157 studies are essential in the optimization of downstream processing leading to multiple-
158 compound production in a biorefinery concept, which could ultimately enhance the
159 economic viability.

160 **1.2 Properties and Potential of *Phaeodactylum tricornutum***

161 Among marine diatoms, *Phaeodactylum tricornutum* is one of the species examined to
162 the highest extent and whose genome has been completely sequenced in 2008. It is a
163 marine pennate diatom and belongs to the brown-algae division of Bacillariophyceae of
164 Heterokontophyta. It contains about 36.4% of proteins, 26.1% of carbohydrates, 18.0%
165 of lipids, and 15.9% of ash on dry weight, under ordinary cultivation conditions (Zhang
166 et al., 2018). *P. tricornutum*, growing in brackish to saline water in several locations of
167 the world, owns the peculiar feature to be polymorphic, thus exhibiting three principal
168 morphotypes: oval, triradiate, and fusiform (**Figure 1**). Evidence is also present that a

fourth rarer morphotype exists, called cruciform, favoured by low temperatures, and converting to the oval type through the degeneration of arms (He et al., 2014).

As a consequence of fluctuations in growth conditions, especially culture medium, salinity, pH, and temperature, the cells are subjected to reversible morphological conversions from one form to another. For instance, suboptimal conditions such as low temperature, hyposalinity, low light intensity, and nutrient limitation resulted to stimulate oval cell formation. Song et. al (2020) characterized ten strains of *P. tricornutum* and reported that Mann and Myers' medium favours morphotype transition from fusiform to oval, while the prevalence of fusiform cells was observed in f/2 medium. Biochemical analysis proved that oval morphotype accumulated higher protein and pigments content, whereas lipids and carbohydrates were more abundant in fusiform cells. However, the latter exhibited a higher maximum specific growth rate (0.76 d^{-1} against 0.43 d^{-1}; doubling time 0.92 d against 1.65 d) (Song et al., 2020). Thereby this study opens up the possibility of selectively growing a certain morphotype when specific final characteristics are desired for a particular industrial application. Oval cells are also characterized by harder walls (Young modulus equal to 500 kPa) compared to the other types (100 kPa) (Francius et al., 2008) and by siliceous frustules when silicic acid is included in the growth medium. Nonetheless, silicified substances are not indispensable for *P. tricornutum*, which can effectively reproduce also in absence of silica. Differences have been noted when comparing silicified fractions of the triradiate and fusiform with those of the oval type: fusiform and triradiate cells are characterized by silica bands; while only the oval ones hold silica valves typical of diatoms (Tesson et al., 2009).

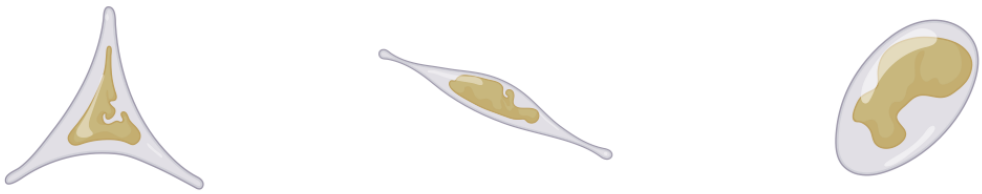

Figure 1. Morphotypes of *Phaeodactylum tricornutum* from left to right: triradiate, fusiform, oval. (Created with Biorender)

198 Among other properties, *P. tricornutum* presents a high ability for the Non-
199 Photochemical Quenching (NPQ) that dissipates the excess light in form of heat. This
200 capacity was tested by using a sinusoidal light scheme for its cultivation and the
201 outcome was that this diatom exhibited minimal indications of photoinhibition. Damage
202 by photoinhibition can be measured as photosynthetic capability by the maximal
203 quantum yield (F_v/ F_m) of photosynthetic system II (PSII), where F_m indicates
204 the maximal fluorescence level and F_v is the variable fluorescence obtained by
205 subtracting F_o (minimal fluorescence) to F_m (Jallet et al., 2016; Murchie and Lawson,
206 2013). The study of Huete-Ortega et al. (2018) shows that light irradiance above 400-
207 500 µmol photons m^{-2} s^{-1} saturated PSII activity of *P. tricornutum*, independently of
208 nitrogen-replete or -deplete conditions. Moreover, the NPQ response was not activated
209 until approximately 200 µmol photons m^{-2} s^{-1} irradiance; therefore, an optimal light
210 intensity of 213 µmol m^{-2} s^{-1} was found for *P. tricornutum* in N-replete mode (Huete-
211 Ortega et al., 2018).
212 An industrially relevant feature of *P. tricornutum* is that it is a fast-growing species,
213 which makes it suitable to be cultivated at a large scale. To date, in Europe, it is
214 cultivated by at least eight companies reaching a yearly production of 4 tons of dry
215 biomass (Araújo et al., 2021). Among them, *P. tricornutum* is exploited for fucoxanthin
216 production by AlgaTechnologies (Israel) and for EPA production by Simris (Sweden).
217 Moreover, *P. tricornutum* extract and EPA-rich oil extract were proposed for
218 authorization as novel food to the European Union, whose evaluations are still ongoing.
219 This diatom presents a strong adaptation to a wide assortment of culture media,
220 including Walnes, f/2, COMBO, M&M, and enriched seawater. It tolerates high
221 pH/light intensities albeit growing also under poor light conditions (Butler et al., 2022).

In addition, it can be genetically transformed, and the employment of different genetic manipulations showed promising results in increasing lipid content. However, the exploitation of diatoms' lipids for biofuel production is far to be economically competitive on the market; thereby, priority should be given to multiple high-value compound production. The valorisation of all biomass components by extracting multiple algae metabolites, can improve the economic feasibility of this value chain and promote their industrial application (Branco-Vieira et al., 2020).

Even if less commercially competitive, healthful substances obtained from microalgae own specific advantages over standard synthetic alternatives: from a chemical point of view, synthetic molecules are only present in specific isomers, which are normally much less effective than natural versions for certain applications, such as in artificial milk, dietary supplements or fish pigment enhancers (Enzing et al., 2014). PUFAs such as EPA and DHA have been shown to improve eye health, and brain development, and perform cardiovascular and inflammatory disease prevention, anti-aging function, and treatment of psychiatric disorders. Currently, deep ocean fish oil represents the primary feedstock for EPA and DHA production; however, unpleasant smell, environmental impacts to the marine ecosystem due to overfishing, heavy metals toxicity, and considerable purification needs demanded sustainable fatty acids production alternatives (Kadalag et al., 2021). Moreover, only 0.2 million tons of EPA/DHA are obtained from fish sources, in the face of 1.3 million tons required for the world population, given the 500 mg/day intake recommended by the World Health Organization (Wang et al., 2021). Hence, further studies to increase fatty acids accumulation in microalgae biomass are needed to facilitate their industrial application. Fucoxanthin also exerts multiple pharmacological bioactivities including anti-inflammatory, anti-obesity, anti-

246 diabetic effects, anti-cancer, and antioxidant (Song et al., 2020). Anti-tumor
247 bioactivities were determined also in chrysolaminarin (Zhang et al., 2018).

248 **2. Cultivation strategies**

249 Microalgae are generally considered to be obligate photoautotrophs, by using sunlight
250 and converting CO_2 to reduced carbon, thus producing oxygen and chemical energy
251 through photosynthesis (Penhaul Smith et al., 2020). This encompasses a series of
252 biochemical redox reactions which convert light energy into chemical energy in the two
253 photosystems, PSI and PSII. The ATP and the reducing power (NADPH), resulting
254 from the electron transport chain, are then metabolized in the Calvin–Benson–Bassham
255 cycle (CBB) by the Rubisco enzyme (Villanova et al., 2017). Nevertheless, many
256 microalgae can assimilate organic nutrients and grow in the dark by respiration or
257 fermentation of exogenous sugars through *heterotrophy*. If the species can switch
258 between heterotrophy and *phototrophy*, or employs both respiration and photosynthesis,
259 then the cultivation is carried out in *mixotrophy*. However, the provision of an organic
260 carbon compound will induce a variation in the cell carbon partitioning with relative
261 consequences on metabolic pathways, growth phase, and final biochemical composition
262 (Penhaul Smith et al., 2020).
263 Even if microalgae production through phototrophy could be a cheap process since only
264 light energy is exploited, this cultivation mode entails some limitations such as the
265 scarce maximum biomass production achievable because of self-shading effects and the
266 subsequent drawbacks in optimizing temperature control, gas/liquid ratio, and light
267 penetration. On the other hand, mixotrophy is considered a viable alternative to obtain
268 high biomass productivity, considering the lower demand for light penetration.
269 Moreover, by employing cheap and easily accessible organic carbon sources, including

wastewaters, the economic feasibility of the process can be even further enhanced (Villanova et al., 2021). The selection of the cultivation mode, and subsequently of the carbon sources in the case of mixotrophy and heterotrophy, depends on the species and the bioproducts of interest. Indeed, if PUFAs production through heterotrophy is feasible, the same can not be achieved for pigments since the production of photosynthesis-related compounds is strictly associated with the presence of light and it is thereby nullified in heterotrophic cultures (Cerón-García et al., 2013, 2005). In addition, some species could not be able to operate heterotrophic growth through dark sugar fermentation, which is the case of *P. tricornutum* which can be grown heterotrophically only upon metabolic engineering (Villanova et al., 2021).

2.1 Phototrophic cultivation of *Phaeodactylum tricornutum*

Several photobioreactors (PBRs) types such as flat-plate, bubble-columns, and tubular, have been designed and tested to cultivate *P. tricornutum* phototrophically. Among these, flat-panel configurations have proven to accomplish low shear stress and adequate irradiation which ultimately resulted in higher biomass, EPA, and fucoxanthin productivities. Illumination constitutes a primary affecting element in biomass production and biochemical composition, together with light wavelength and light:dark cycle. The increase of light intensity usually involves the rise of the growth rate until it reaches a saturation value. Nonetheless, above this saturation value, the growth is inhibited by the production of harmful substances (i.e., ROS), involved in the photoinhibition process, which eventually cause a decrease in biomass productivity (Villanova et al., 2021). Generally, the photosynthetic efficiency in microalgae grown in phototrophic conditions is lower than theoretically achievable values, due to the complex nature of the culture system, in which various parameters influence differently

294 the growth and the biochemical composition, resulting in countertrend effects. (Butler et
295 al., 2020). Maximum biomass productivities achieved with *P. tricornutum*, and the
296 productivity of different target compounds obtained in phototrophic cultures are
297 reported in **Table 1** and **Table 2,** respectively.
298

Strain	Medium	Photobioreactor design	Maximum biomass productivity	Reference
UTEX 640 and UTEX 646	f	Green wall panel III (≤40 L) outdoor	17.80 g m^{-2} day^{-1} (nitrogen-replete culture)	(Gilbert-López et al., 2015)
FACHB-Collection	f/2	Indoor bubble columns photobioreactors (3 L)	227.09 mg L^{-1} day^{-1}	(Rodolfi et al., 2017)
UTEX 640	ASW	Outdoor parallel photobioreactors (51 L)	> 0.3 mg L^{-1} day^{-1}	(Song et al., 2014)
		PVC circular outdoor pond	~ 0.15 mg L^{-1} day^{-1}	
EPSAG-Collection	f/2	Greenhouse PBR phytobags (3000 L)	7.62 g m^{-2} day^{-1}	(Silva Benavides et al., 2013)
CCAP 1055/1	Cell-Hi JWP	Indoor Airlift glass tubular photobioreactor (ALR) PhycoLift (8 L)	1.57 g L^{-1} day^{-1}	(Wang et al., 2018)
		Outdoor Airlift glass tubular photobioreactor (ALR) PhycoLift (8 L)	0.93 – 1.13 g L^{-1} day^{-1}	

Table 1. Biomass productivity of *P. tricornutum* strains in various photosynthetic systems.

Product class	Product	Strain	Product yield / productivity	Operational conditions	Reference
Lipids	EPA	EPSAG-Collection	280 mg m^{-2} day^{-1} 3.68% DW	Greenhouse PBR phytobags (3000L)	(Butler et al., 2022)
		CCAP 1055/1	3.31% DW	Airlift glass tubular photobioreactor (8 L)	(Wang et al., 2018)
	TAG	UTEX 640	58.5 mg L^{-1} day^{-1} 45% DW	Outdoor green wall panel III (≤40 L)	(Butler et al., 2022)
Carbohydrates	Chrysolaminarin	CAS	94 mg L^{-1} day^{-1} 14% DW	Indoor flat-plate (50 L)	(Rodolfi et al., 2017)
Pigments	Fucoxanthin	CAS	4.7 mg L^{-1} day^{-1} 0.7% DW	Indoor flat-plate (50 L)	(Gao et al., 2017)
		CCAP 1055/1	1.33% DW	Airlift glass tubular photobioreactor (8 L)	(Gao et al., 2017)

Table 2. Productivity of different target products from *P. tricornutum* strains in phototrophic cultures.

2.1.1 Influence of culture parameters on lipids production and composition

The content of bioactive molecules in microalgae can be remarkably affected by the culture conditions and the biochemical composition of biomass is subjected to fluctuations during the culture period. Qiao et. al (2016) performed phototrophic laboratory cultures of *P. tricornutum* Bohlin, from the Microalgae Culture Center (MACC), Ocean University of China, in f/2 medium in 500 mL flasks, irradiated by LED lamps working on a 14:10 h light:dark photoperiod and shaken at 100 rpm. The authors studied the effect of the variation in salinity (15; 20; 28; and 35 ppt), nitrogen concentration (1.24; 12.35; 24.70; and 49.40 mg L^{-1}), light intensity (photosynthetic photon flux density PPFD) (50, 100 and 150 μmol m^{-2} s^{-1} with 14:10 h light:dark photoperiod) and temperature (15; 20; 25°C) over fatty acid composition. Under N-limitation conditions, *P. tricornutum* produced greatly MUFAs and saturated fatty acids at the expenses of PUFAs. However, this nutrient starvation also led to a significant decrease in biomass concentration. The lowest salinity caused the lowest total FAs production, but no variation in FAs composition was observed as a function of salinity. DHA accumulation was increased by rising irradiance, while DHA, EPA, and PUFAs decreased with increasing temperature. N-starvation, low salinity, and low temperature promoted the production of DHA at the expense of EPA. Ultimately, the best biomass productivity was achieved for 28 ppt of salinity, 12.35 mg L^{-1} concentration of nitrogen, 50 μmol m^{-2} s^{-1} light intensity, and 20°C (Qiao et al., 2016).

Even if nitrogen limitation can improve lipid contents in microalgae, higher biomass productivity can be reached in higher nitrogen concentrations; an optimum of 32.09 mg/L $NaNO_3$ was found to be most favorable for algal biomass productivity (Yodsuwan et al., 2017).

An indoor flat-plate photobioreactor (50 L) was used to test and study the biochemical composition of *P. tricornutum* obtained from the Institute of Oceanography, Chinese Academy of Sciences. Two different nitrogen concentrations were assayed: 14.5 mmol L^{-1} (HN) and 2.9 mmol L^{-1} (LN) of KNO_3. Continuous illumination provided by cool white fluorescent lamps at an irradiance of 300 μmol m^{-2} s^{-1}, 25 ± 1°C and air bubbling (enriched with 1% of CO_2) were the operative conditions for the 12 days of growing. The maximum biomass concentration was obtained under HN amounting to 4.05 g L^{-1}. However, lipid accumulation was accelerated under the LN condition, which achieved 42.48% DW of total lipids (TLs), compared to 36.69% in HN. Regarding the lipids profile, at first, glycolipids were the components more abundant of TLs under both HN and LN. Neutral lipids, mainly TAGs, increased as culture time proceeded and amounted to 63.84% and 75.7% of TLs in HN and LN conditions. It was also noted that as the growth period was protracted, the proportion of PUFAs experienced a decrease, while saturated fatty acids increased.

Arachidonic acid (C20:4), EPA (C20:5), oleic acid (C18:1), linoleic acid (C18:2), palmitic acid (C16:0), palmitoleic acid (C16:1), and myristic acid (C14:0) were the fatty acids detected in most abundance. C16:1 increased from 15.55% to 38.67% of total fatty acids in HN treatment and from 15.40% to 40.96% in LN. C20:5 content drastically declined with culture time (Gao et al., 2017).

Besides medium composition, important design considerations for the cultivation system should be accounted for. For example, when designing a photobioreactor system, a parameter to be considered as influencing growth performances is the Gas-Liquid Ratio (GLR). A certain value of gas-liquid ratio can assure the proper culture mix, thus preventing sedimentation, increasing the mass transfer, facilitating the

assimilation of nutrients by the cells, and forcing them to shift from dark to light zone. However, an excessive degree of the GLR may damage cells due to mechanical shear stress and cause the evaporation of the culture medium. *P. tricornutum* from the freshwater algae culture collection of the Institute of Hydrobiology in China (FACHB-Collection) was grown testing different GLR values to find the optimum experimental condition. A GLR of 1.5 vvm allowed to reach 0.5 d^{-1} as specific growth rate and 227.09 mg $L^{-1}d^{-1}$ as biomass productivity, which were the highest values obtained along with the highest lipid productivity of 48.48 mg $L^{-1}d^{-1}$. (Song et al., 2014).

2.1.2 Influence of culture parameters on fucoxanthin production

Fucoxanthin accumulation in *P. tricornutum* was studied as influenced by several experimental factors. In particular, it was found to be decreasing as the culture time was prolonged, and the decline was accelerated by nitrogen deficiency (Gao et al., 2017). In contrast, low light intensities have been found to promote higher production of fucoxanthin. For instance, a light intensity of 100 μmol m^{-2} s^{-1} on *P. tricornutum* (CS-29) supplied by the Australian National Algae Culture Collection (ANACC), cultured in 5 L photobioreactors with f/2 medium at 25 ± 3 °C, resulted in a greater specific fucoxanthin concentration (42.8 ± 19.5 mg g^{-1}) than at 210 μmol m^{-2} s^{-1} (9.9 ± 4.2 mg g^{-1}). This behaviour can be explained by considering that the production of this light-harvesting pigment is boosted when low light conditions are applied. Conversely, as the light intensity increases, fucoxanthin's content decreases on behalf of photoprotective pigments. In addition, the composition of growth medium was examined as affecting the growth and fucoxanthin accumulation, after choosing a working irradiance of 150 μmol m^{-2} s^{-1}. For this purpose, besides f/2 standard recipe, two other media were prepared: 10 × f/2, where all nutrients' concentrations were increased by 10-fold, and

f/2 with only nitrate concentration increased by 10-fold. Cells cultivated with the first enriched medium resulted in a 2-fold final dry cell weight (0.59 ± 0.10 g L^{-1}) compared to standard f/2 medium (0.29 ± 0.03 g L^{-1}), but a lower specific growth rate. Fucoxanthin concentration was remarkably increased by the medium with nitrate supplementation reaching the maximum of 59.2 ± 22.8 mg g^{-1} dry algae, against 23.2 ± 7.0 mg g^{-1} produced in f/2 medium and 26.7 ± 13.1 mg g^{-1} in 10 × f/2 medium. These results clearly indicate that fucoxanthin accumulation in *P. tricornutum* is promoted by supplementation of nitrate in culture medium, even if further investigations are required to understand the processes by which this happens (McClure et al., 2018). Yet, it is worth emphasizing that cellular growth and fucoxanthin production are not directly related as the best culture conditions do not always lead to the highest fucoxanthin production (Gómez-Loredo et al., 2016).

2.1.3 Influence of culture parameters on carbohydrates production

In all algae species, carbohydrates represent the first photosynthetic product exiting the Calvin–Benson cycle, acting as precursors for all cell components. Initially, carbohydrates' production is significant and then decreases due to their conversion into other metabolites required by cells. The evolution of total carbohydrate and chrysolaminarin contents in *P. tricornutum* was studied by Gao et. al (2017), who concluded that major amounts of carbohydrates are obtained when cells are in their exponential growth phase, rather than in cells entering the stationary phase. Besides, N-deplete conditions have proven to induce a fast accumulation of these metabolites. The maximum carbohydrate and chrysolaminarin amounts, under 14.5 mmol L^{-1} of nitrogen, were 21.2% and 17.1% of DW, respectively (Gao et al., 2017).

Carbohydrates' accumulation is favoured also by higher light intensities since their degradation takes place in the dark. This was confirmed also by Chauton et al. (2013) who found that carbohydrate content in *P. tricornutum* (CCMP 2561) increased with prolonged illumination or extended light phase considering that the phase in which they are produced is longer, while the phase associated with carbohydrates consumption (darkness) is reduced. Moreover, carbohydrates concentration was increased in cells grown in N-depletion rather than in P-depletion. (Chauton et al., 2013). The study of daily fluctuation in biomass composition of *P. tricornutum* CCAP 1055/1 performed by Jallet et al. (2016) allowed also to state that carbon dislocation between diverse metabolites varies remarkably during the light: dark cycle. For instance, biomass was found richer in TAGs and carbohydrates at the end of the light phase if compared to its start, while the reverse condition resulted in proteins. These daily trends should be accounted for when selecting the right moment to harvest, extract a specific metabolite, or for measuring daily productivity (Jallet et al., 2016). Similar results were obtained on the same strain by Caballero et al. (2016) who presented an experimental procedure to simultaneously characterize and resolve insoluble, soluble reducing, and soluble nonreducing carbohydrates from *P. tricornutum*, to study the carbon partitioning during nitrogen replete and nitrogen deplete conditions. They confirmed, through compositional and structural analysis, the hypothesis that chrysolaminarin belongs to the soluble nonreducing carbohydrate portion.

Moreover, by comparing laminarin and chrysolaminarin structures, they observed that *P. tricornutum*' s chrysolaminarin is smaller and lightly branched. During nitrate starvation, chrysolaminarin was produced to store only 4.9–6.0% of cellular carbon, which is definitively lower if compared to the TAG accumulation amounting to 43–

50%. This result led the authors to the conclusion that chrysolaminarin is not the preferred storage product during nitrogen limitation. Ultimately, nutrient replete conditions and high irradiance allowed high accumulation of chrysolaminarin in *P. tricornutum*, which occurs at night in a 12:12 light:dark cycle, while its consumption is completed by dawn (Caballero et al., 2016).

2.2 Mixotrophic cultivation of *Phaeodactylum tricornutum*

Mixotrophic cultivation mode, occurring when an organic carbon source is supplied concurrently with the use of light, allows benefiting from the main advantages of both phototrophy and heterotrophy. This cultivation procedure can hence lead to high biomass productivity while enriching microalgal biomass with the profitable photosynthesis-related metabolites, which are normally missing in heterotrophic mode (Cerón-García et al., 2013).

It is noteworthy that mixotrophy demands proper uptake proteins that enable the metabolism of the chosen carbon source. If their upregulation and expression employ too much time, a lag phase in population growth may result (Penhaul Smith et al., 2020). Nevertheless, compared to phototrophic cultures, growth rates, and biomass production increase thanks to the synergy established between light and the organic source. In mixotrophic cultures, the cellular composition varies according to the period that cells spend in dark and enlightened areas, or, in other words, the respective contribution of the heterotrophic and phototrophic metabolisms to the total growth.

In high-density cultures, occurring for high cell concentrations, the light fails to reach efficaciously all cells so that the contribution of the phototrophy to the overall growth rate decreases and the consumption of the organic carbon source becomes sustaining the growth. Even if mixotrophy is a promising alternative culture method to improve

biomass productivity, its potential and applicability can vary according to the target metabolite. An optimal balance exists indeed between phototrophic and heterotrophic growth for the optimal productivity of every specific compound (Cerón-García et al., 2013, 2005, 2000). Recent studies tried to unravel the molecular function of mixotrophy by concluding that the optimized photosynthetic efficiency in diatoms is achieved through cooperation between mitochondria and plastids. Actually, the synergic actions of these organelles, through exchanges of ATP and NADH, enable close coordination between respiration and photosynthesis, thus simultaneously improving the uptake of light and organic carbon during mixotrophy (Villanova et al., 2017).

Several organic compounds such as glycerol, acetate, glucose, fructose, starch, and glycine can be used to cultivate the model diatom *P. tricornutum*, and some studies tested this capacity through the years. **Table 3** shows maximum biomass productivities and concentrations arising from the use of different organic sources on *P. tricornutum* under mixotrophic conditions. In **Table 4** the maximum productivities of diverse compounds obtained from *P. tricornutum* in mixotrophy conditions are collected.

Strain	Organic carbon source	Maximum biomass productivity	Maximum biomass concentration	Reference
UTEX 640	Glucose 5 g L^{-1}	10.70 mg L^{-1} h^{-1}	2.01 g L^{-1}	(Cerón-García et al., 2005)
	Acetate 0.05 M	13.2 mg L^{-1} h^{-1}	1.15 g L^{-1}	
	Glycine 0.01 M	11 mg L^{-1} h^{-1}	2.46 g L^{-1}	
	Starch 1 g L^{-1}	11.3 mg L^{-1} h^{-1}	1.79 g L^{-1}	
	Lactic acid 0.005 M	7.73 mg L^{-1} h^{-1}	2.18 g L^{-1}	
	Glycerol 0.1 M	17.5 mg L^{-1} h^{-1}	2.99 g L^{-1}	
CCAP 1055/1	Glycerol 0.05 M	-	11.55 g L^{-1}	(Cerón-García et al., 2005)
UTEX 640	Fructose 0.02 M	6.8 mg L^{-1} h^{-1}	8.2 g L^{-1}	(Villanova et al., 2021)
	Glycerol 0.1 M	14 mg L^{-1} h^{-1}	14 g L^{-1}	

Table 3. Maximum biomass productivity and concentration of *P. tricornutum* on different organic sources under mixotrophic cultures.

Product	Strain	Organic carbon source	Product yield / productivity	Reference
EPA	CCAP 1055/1	Glycerol	9.51 ± 0.13 mg L^{-1} d^{-1}	(Butler et al., 2022)
Fucoxanthin			1.97 ± 0.34 mg L^{-1} d^{-1}	
FAMEs			51.96 ± 0.61 mg L^{-1} d^{-1}	
EPA	UTEX 640	Glycerol	8.56 mg L^{-1} d^{-1}	(Cerón-García et al., 2005)
		Glycerol 0.1 M + Urea	11.53 mg L^{-1} d^{-1}	
Total Pigments		Lactic acid	4.45% DW	
Chlorophylls		Lactic acid	3.79% DW	
Carotenoids		Starch	1.04% DW	

Table 4. Productivity of different target products from *P. tricornutum* strains in mixotrophic cultures.

2.2.1 Glycerol

The effect of glycerol on *P. tricornutum* metabolism has been assessed via transcriptomics, metabolomics, metabolic modelling, and physiological studies. Results point out that carbon-storage, central-carbon, and lipid metabolism are all affected by the presence of this compound. In metabolic pathways of *P. tricornutum,* glycerol converts to glycerol phosphate, through the action of glycerol kinase, which constitutes the precursor for TAG synthesis, and to dihydroxyacetone phosphate, through the action of glycerol-3-phosphate dehydrogenase, in the glycolysis and pentose phosphate pathway (PPP), thus influencing the central-carbon metabolism. In the case of phototrophy, the diatom's carbon requirement is instead satisfied by the consumption of the inorganic carbon source occurring in the Calvin cycle, characterized by higher enzymatic and light energy costs. The supply of glycerol simulates the characteristic effects of N-starvation on lipid production, contributing to the triacylglycerol and fatty acid accumulation. Nevertheless, unlike nitrogen-deplete conditions which affect biomass productivity, the presence of glycerol neither decreases photosynthetic ability nor diatom's growth (Villanova et al., 2021, 2017).

Cerón-García et al. (2000) reported the EPA production from *P. tricornutum* UTEX 640 strain under mixotrophic conditions using glycerol and studied the effect of different glycerol concentrations (0.005; 0.01; 0.05; and 0.1 M) and subsequent additions of glycerol and ammonium chloride on growth kinetics, biomass productivity, and fatty acid profiles. The authors used one-liter flasks with enriched seawater medium that were sparged with filter-sterilized air (0.22µm Millipore filter) at 0.1 v/v min^{-1} to mix the suspension. The cultures were continuously illuminated at an irradiance of 165 µmol photons $m^{-2}\,s^{-1}$ at a temperature of 20 ± 0.5°C. The optimal initial concentration of

498 glycerol was determined as 0.1 M, which resulted in maximum biomass productivity
499 and concentration of 17.5 mg L^{-1} h^{-1} and 2.4 g L^{-1}, respectively. However, a lag phase
500 lasting for the first 160 h of growth was observed for cultures grown with higher
501 glycerol concentrations; they indeed maintained a biomass concentration below that of
502 the control (in absence of glycerol). No lag phases were observed for lower glycerol
503 concentrations, which indicates that this physiological response was due to an
504 adaptation period to a high glycerol environment. Once the optimal glycerol
505 concentration was established, a fed-batch culture was performed by operating
506 sequential additions of ammonium chloride and glycerol. In these conditions, the
507 resultant EPA productivity equal to 33.5 mg L^{-1} d^{-1} was recorded as the highest
508 obtained (Cerón-García et al., 2000).
509 In another study, different pilot-scale photobioreactors systems were used for the
510 cultivation of *P. tricornutum* UTEX 640 strain, grown in fed-batch and under
511 mixotrophic conditions: outdoor vertical bubble column (BC), draft-tube airlift (DT),
512 and split-cylinder (SC), each of 60 L working volume. The diatom was grown on a
513 modified Ukele medium supplemented with an initial 0.1 M of glycerol, with
514 subsequent additions of nutrients (glycerol, ammonium, urea), which instantaneously
515 improved the growth rate. Best performance in terms of maximum biomass
516 concentration was reached in SC photobioreactor with 25.4 g L^{-1}. The supplied organic
517 nutrient did not significantly affect carotenoids and chlorophylls content since they
518 remained at 0.4-0.8% and 1.5-2.0% DW respectively. EPA content raised to 3% DW
519 reaching a productivity of 56 mg L^{-1} d^{-1} (Fernández Sevilla et al., 2004).
520 Furthermore, *P. tricornutum* (CCAP 1055/3 axenic strain) was cultivated in a 250 mL
521 Erlenmeyer using an artificial seawater medium enriched with extra nitrogen and

phosphorus (ESAW) to obtain 0.47 g L^{-1} N and 0.03 g L^{-1} P. Cultures were conducted in phototrophy with N-depletion (PHOT-N) shaken at 100 rpm and 20°C, under a light intensity of 40 µE m^{-2} s^{-1} with a 12h:12h light:dark cycle. Regarding mixotrophic tests, glycerol was supplemented to the medium to reach a final concentration of 50 mM in both N-replete and N-deplete tests. Glycerol enhanced biomass production by 2-fold compared to growth in PHOT medium, favoring nitrogen and phosphate consumption, and did not inhibit the photosynthetic ability. Moreover, its presence affected cellular lipid content by increasing TAG accumulation in both nitrogen-replete and starved cells. These results suggest that glycerol act as TAG-booster by providing the glycerol backbone and the acyl groups required for TAG assembly (Villanova et al., 2017).

In a follow-up study, the optimized ESAW medium (added with sodium bicarbonate and extra nitrogen and phosphorous) was used to grow *P. tricornutum* (CCAP 1055/3 strain) in mixotrophy with glycerol (4.6 g L^{-1}) in a 2 L photobioreactor sparged continuously with air at a flow rate of 0.5 L min^{-1} and under a controlled temperature of 20°C. Cultures were continuously illuminated by a variable light intensity of 70 to 300 µmol m^{-2} s^{-1}. These fluorescence studies were conducted to determine the light dependency of NPQ: a value of 400 µE was found as sufficient to obtain the maximum value of fluorescence, without provoking damage to the photosynthetic system. The biomass concentration was found to increase by a factor of 9 in the optimized medium compared to the conventional enriched seawater medium. Moreover, both biomass quantity and quality were enhanced by the provision of the organic and inorganic ($NaHCO_3$) carbon sources. Both respiration and photosynthesis performances were improved in these mixotrophic tests, confirming the energetic coupling of these two

metabolic processes. Ultimately, the optimized medium allowed to obtain higher productivity in biomass and lipids compared to other studies (Villanova et al., 2021).

2.2.2 Other carbon sources

Other carbon sources tested on *P. tricornutum* under mixotrophic conditions are acetate, glucose, fructose, starch, glycine, and lactic acid. Acetic acid is metabolized bonded to acetyl-CoA protein and carried in the glycoxysome, by entering the TCA cycle (tricarboxylic acid cycle) in the mitochondria, or directly used for fatty acid biosynthesis, which provides an increase in respiration and carbohydrate accumulation (Penhaul Smith et al., 2020).

P. tricornutum UTEX-640 strain growth was tested on different substrates at diverse concentrations in fed-batch and discontinuous modes (fed-batch only for glycerol). The nutrients assayed were glucose (0.5 to 5 g L^{-1}), acetate (0.005 to 0.1 M), glycerol (0.005 to 0.1 M), lactic acid (0.005 to 0.1 M), starch (0.5 to 5 g L^{-1}), glycine (0.005 to 0.02 M). Filter-sterilized air at 0.1 vvm was used to mix and aerate the cultures. These were constantly irradiated at 165 µmol m^{-2} s^{-1} and maintained at 20 ± 0.5°C. The authors studied biomass productivity and biochemical composition. Experiments with acetate indicated that growth inhibition occurs above 5 mM: growth was decelerated, and biomass concentration and productivity declined. Contrastingly, growth was stimulated by all starch concentrations tested, and only a slight inhibitory response was reported for concentrations above 2 g L^{-1} of starch. Lactate consistently promoted growth in most experiments, gaining the maximum biomass concentration for 5 mM; however, a possible inhibition was detected for 0.1 M of lactate which induced the decrease of final biomass concentration. All concentrations of glucose resulted in a stimulating effect for the growth, although not very intense. The study of the organic substrate as influencing

metabolites production led to varied results. If lactate, glycine, glycerol, and starch stimulated the biosynthesis of total pigments on one side, an opposite effect was observed for glucose. Same trends were found for chlorophyll contents. EPA productivity was remarkably influenced by nutrient source: lactate and glucose increased EPA content, while starch decreased it. Glycine had no significant influence on cellular EPA concentration (Cerón-García et al., 2005). Another study compared the mixotrophic cultivation of *P. tricornutum* UTEX-640 strain grown on fructose and glycerol. These cultures were performed in bubble photobioreactors (2 L) in fed-batch mode, with enriched seawater as medium, temperature maintained at 20 ± 0.5°C, use of CO_2 for pH control, and a sparging air flow rate of 1.5 vvm. Diverse nutrient-supply procedures, along with a sequential increase of irradiance (280 to 750 µE m^{-2} s^{-1}) were assayed. At first, the batch mode was employed to initiate the cultures; then, when cells enter the stationary stage, the nutrient supply and/or irradiance increment was executed. During the first part of the cultivation (117 h), the biomass concentration raised similarly to phototrophic control, and no fructose was consumed, indicating that high percentages of inorganic carbon (CO_2 and HCO_3^-) can force the diatom to grow phototrophically, which, in turn, inhibits the assimilation of organic carbon. The consumption of fructose was initiated when the CO_2 injection for pH monitoring was discontinued; consequently, cell growth and biomass concentrations immediately raised upon the organic C source consumption. Despite this, final biomass concentrations of mixotrophic cultures with fructose were lower than the phototrophic control (Cerón-García et al., 2013).

2.2.3 Waste effluents

Recently, industrial, agricultural, and municipal wastewater effluents have been efficaciously tested for microalgae cultivation and production. There is no lack of studies testing the growth performances of *P. tricornutum* by adding wastewater effluents to the culture medium. The recovery of nutrients contained in these types of effluents can reduce the cost of fertilizers and has the advantage of reducing the amount of nutrient-rich digestate to dispose of, while eventually lowering the costs associated with microalgae cultivation thus promoting a circular economy approach (McDowell et al., 2020; Su et al., 2020). *P. tricornutum* batch cultures were grown mixotrophically with glycerol as carbon source and ultrafiltered digestate (UF) from a biogas plant as nitrogen source, testing different concentrations of glycerol (0.02; 0.03; 0.04 M). In their study, the strain SAG1090-1a was cultivated in a 0.5 L photobioreactor at 25°C, at a constant air flux of 10 L min^{-1}, 312 µmol m^{-2} $s^{-1,}$ and a 12h:12h photoperiod. CO_2 injection was used to control pH at 8 and the f/2 culture medium was added with UF and different concentrations of glycerol. The highest biomass concentration reached was 4.96 g L^{-1} corresponding to an addition of 0.04 M of glycerol. Biomass productivity increased by 1.29 and 1.60 times, compared to the control, with 0.03 M and 0.04 M of glycerol respectively. The balance study performed on nitrogen demonstrated that UF supplement increased nitrogen availability, thus promoting algal growth and protein accumulation. Regarding diatom's biochemical properties, the highest glycerol concentrations caused a decline in protein content due to N limitations, while lipid content did not show variability as UF and/or glycerol were provided. However, the fatty acid profile changed compared to the phototrophic control: under mixotrophic conditions, saturated fraction increased at the expense of ω-3 and PUFAs contents. The supply of glycerol was found to switch the metabolism to carbohydrate production,

whose content displayed a remarkable increase. Nevertheless, the authors reported that carbohydrates' increase and proteins' decrease were also a consequence of nitrogen starvation induced by microbial competition, which forced the diatom towards carbohydrates accumulation (Su et al., 2020).

Anaerobic digestate also represents a rich source of nitrate, ammonium, phosphorous, and trace micronutrients required for microalgae growth, although high concentrations of ammonium (> 80-100 mg L^{-1}) can potentially inhibit it. Three AD plants were selected to investigate how their effluents affect the biochemical profile of *P. tricornutum*: (1) cow slurry and grass silage (CW); (2) pre-consumer food waste (FW); (3) pig slurry and grass silage (PW). 5 L photobioreactors irradiated by 170 µmol m^{-2} s^{-1} at 20 ±1 °C, were used for the trials. *P. tricornutum* CCAP 1052/1B strain was cultivated in digestate media of different concentrations obtained by supplementing 1%, 3%, or 6% v/v liquid digestate stream to seawater. All these media provided enough nourishment for *P. tricornutum* cells, whose growth rate was similar or higher to the ones reached in the f/2 control. Initial lag phases of cell adaptation were observed for higher concentrations of effluent. All concentrations of CW and FW resulted in a considerable enhancement of crude protein production compared to the control. CW 1% produced microalgae richer in ω-3 and EPA, compared to PW 1%, but similar to control. Major quantities of fatty acids DW were obtained in microalgae grown in lower levels of digestate concentrations, being CW 1% and PW 1% the ones to produce the highest values of total fatty acids. Ultimately, CW 1% digestate has proved to be the best digestate in terms of the total fatty acids and proteins accumulation (McDowell et al., 2020).

639 The suitability of this diatom to grow also in municipal wastewater (MW) mixed with
640 seawater (SW) in compositions MW:SW = 1:1 and MW:SW = 2:1 was tested
641 successfully. *P. tricornutum* CCMP632 strain was grown at 18 °C and 120 μmol m^{-2} s^{-1}
642 under a 12h:12h photoperiod. The final biomass increased by about 40% compared to
643 f/2 control, indicating the possibility of using this type of effluents to grow the species.
644 Growth performances were further enhanced in cultures supplemented with air aeration,
645 which also facilitated lipids accumulation. MW: SW=1:1 and f/2 medium tests allowed
646 to obtain the highest quantities of lipid (34.4% and 35.5%); furthermore, MW: SW=1:1
647 condition accomplished also the highest lipid productivity (33.20 mg L^{-1} day^{-1}) (Wang
648 et al., 2019). Besides the employment of wastewater effluents, the recycling of CO_2 flue
649 gases for growing microalgae represents a further step towards the exploitation of waste
650 resources in a circular economy perspective. Simonazzi et al. (2019) evaluated the
651 viability of employing both waste CO_2 and a pre-treated digestate to cultivate *P.*
652 *tricornutum* and optimize growth and ω-3 productivity in the successive scale-up.
653 Biomass productivity and accumulation of PUFAs were not altered when using waste
654 CO_2. P. *tricornutum* growth was resulted completely supported by the pre-treated
655 digestate and waste CO_2, without the risk of inhibition, to a final biomass density of 1-
656 1.2 g L^{-1}. The biochemical composition of resulted biomass after 15 days of culture
657 was: proteins 36-37%, lipids 34-35%, and polysaccharides 5-6%. The authors reported
658 no differences between biomass grown with flue gas and biomass grown with pure CO_2.
659 (Simonazzi et al., 2019).
660 Other research has also proved the opportunity of growing diverse microalgae species
661 on such effluents, thus potentially reducing the high costs necessary to sustain their
662 industrial production, in terms of nutrient needs (representing 30–40% of operating

costs). At the same time, this solution would allow to purify wastewater effluents and eventually dispose of CO_2 off-gas thus also promoting climate change mitigation, through an economic and environmentally friendly approach. This would be advantageous also for saving money required to recycle and depurate waste streams by removing nutrients (Wang et al., 2019). However, it should be underlined that the chemical profile and complex composition of the effluent will strongly influence the resultant biochemical composition of microalgal biomass, thus influencing its downstream valorisation pathway and possible applications (McDowell et al., 2020). Moreover, with regards to CO_2 streams, the presence of the typical substances constituting flue gases such as NOx, SOx, and heavy metals, should be controlled due to the possibility of culture medium acidification, harmful to the cells, and the bioaccumulation of toxic compounds in the resulting biomass, which eventually compromises its quality and subsequent applicability (Simonazzi et al., 2019).

3. Extraction of value-added products from *Phaeodactylum tricornutum*

Among microalgae species, diatoms are indicated as an auspicious feedstock for the biotechnology sector, since multi-product and fractionation procedures would be able to launch new production chains in different industrial fields (Savio et al., 2020). Although the products recoverable from microalgae are highly profitable from an economic perspective, their industrialization still struggles to establish on the market. Among the reasons, high investments required for downstream purification steps contribute significantly. Moreover, these conventional processes making use of a huge quantity of organic solvents, produce a heavy impact on the environment. Lipid fraction from microalgal biomass has been usually extracted by employing toxic solvents such as chloroform, n-hexane, diethyl ether, methanol, and their mixtures. Therefore, extensive

687 studies have been conducted on the optimization of extraction technologies and
688 especially on the design of new protocols excluding the use of toxic solvents to increase
689 efficiency and sustainability, reduce waste production, and decrease energy
690 consumption. Some green extraction techniques complying with these requirements are
691 Supercritical Fluid Extraction (SFE), Pressurized Liquid Extraction (PLE), Ultrasound-
692 Assisted Extraction (UAE), Microwave-Assisted Extraction (MAE), Pulsed Electric
693 Field (PEF), Enzymatic-Assisted extraction (EAE), and alternative solvents like deep
694 eutectic solvents (DES), and ionic liquids (ILs). Briefly, UAE and MAE make use of
695 generally recognized as safe solvents (GRAS) such as water and ethanol, while
696 enhancing and boosting their extractive capacity, also reducing operating temperature,
697 extraction time, and solvent consumption. During ultrasonication, high-frequency
698 acoustic waves cause a cavitation effect, which culminates in the cell disruption by high
699 shear forces. MAE instead consists in transferring energy to the solution, through the
700 concurrence of dipole rotation and ionic conduction mechanisms. Polar molecules, such
701 as the water inside the cells, absorb the energy and heat up rapidly causing the pressure
702 inside the cell to increase till the cell ruptures and releases cell compounds (Günerken et
703 al., 2015; Zhou et al., 2019). SFE employs a determinate solvent (such as CO_2) at
704 pressures and temperatures higher than the critical point (31.2 °C and 73.8 bar for CO_2)
705 that improve its solvent capacity. This technology also offers the possibility to use a co-
706 solvent to modify the overall polarity and selectively extract specific compounds. PLE
707 applies high temperature (but lower than the critical point) and pressures sufficiently
708 high to keep the solvent liquid. In this case, the solvent possesses augmented solubility
709 and lower viscosity which in turn improves mass transfer and permeation into the
710 biomass sample (Gallego et al., 2018). During PEF, an electrical potential throughout

711 the cell wall is originated by the application of an external electric field. In this case,
712 cell disruption is accomplished by electromechanical compression (Günerken et al.,
713 2015). In addition, ionic liquids are emerging as an interesting alternative to fractionate
714 microalgal biomass. These are low melting salts that are generally used to perform soft
715 and selective extractions from both non-disrupted and disrupted biomass while
716 preserving structural integrity and bioactivity of metabolites (Eppink et al., 2021). The
717 extraction of fucoxanthin from *P. tricornutum* biomass (provided by
718 the Microalgae Collection of Ningbo University) was carried out to investigate the
719 effects of a few factors on fucoxanthin's yield. These factors were the solvent used
720 (methanol, ethanol, acetone, water, and ethyl acetate, ethanol-water mixtures from 60%
721 to 100 % v/v), extraction time (15 to 120 min), extraction temperature (4 to 40 °C), and
722 total extraction rounds. The decreasing order of the solvent's performance in terms of
723 fucoxanthin extraction yield was the following: 1) methanol; 2) ethanol; 3) acetone and
724 ethyl acetate. Thereby, better extraction performances were accomplished when using
725 polar solvents. Even if methanol was revealed to be the most efficient for extracting
726 fucoxanthin, also the greener mixture of 70% ethanol-water performed well. The
727 quantity of fucoxanthin extracted was favored by the increase in operating time and
728 temperature. Moreover, the first extraction was enough to obtain about 80% of the total
729 fucoxanthin. Hence, the optimum experimental conditions to mildly extract fucoxanthin
730 from *P. tricornutum* biomass were solvent/solid ratio equal to 40 mL g^{-1}, operating time
731 90 min, 25°C, 70% mixture ethanol-water, and one extraction round. These
732 conditions allowed to have an extract containing both lipids and fucoxanthin. Therefore,
733 this extract was further purified by an ethanol precipitation process at 25°C, which led
734 to an extraction yield of 7.14 ± 0.11 mg g^{-1} with a recovery percentage of 80.04 ±

735 1.18%. (Sun et al., 2022). Gilbert-López et al. performed a comparison between MAE
736 and PLE technologies for extracting value-added compounds from *P.*
737 *tricornutum* freeze-dried biomass provided by Fitoplancton Marino S.L. and studied the
738 effects of temperature, solvent, and extraction time. A factorial Design of Experiment
739 (DoE) sized 3^2 was conducted to investigate PLE performance and optimize
740 experimental conditions. The investigated factors were temperature (50; 110; 170 °C)
741 and ethanol in different percentages (0; 50; 100%). Whereas the 3^3 factorial design for
742 MAE studied the following factors: extraction time (2; 11; 20 min), composition of
743 ethanol (0; 50; 100%), and temperature (30; 100; 170 °C). The response variables for
744 both DoE studies were extraction yield, antioxidant activity (indicated as Trolox
745 equivalent antioxidant capacity TEAC), total carotenoids, chlorophylls, and total
746 phenols content (TPC). For PLE, the temperature was found to have a positive effect on
747 extraction yield, indicating that it improved the mass transfer, and the solvent solubility,
748 while reducing its viscosity, thus promoting the solvent permeation ability. The solvent
749 mixture water-ethanol (50:50) reached higher yields, compared to pure solvents.
750 Whereas higher phenols content and antioxidant activity were found for pure
751 ethanol. The content of carotenoids increased with a higher percentage of ethanol and
752 decreased with the temperature. Regarding MAE process, the extraction time did not
753 show any significant effect on all response variables. Like PLE, the temperature had a
754 favorable influence on extraction yield also in MAE, and the same was observed when
755 water was present in the solvent mixture; the lowest yields were indeed obtained with
756 pure ethanol. Higher phenolic and TEAC content were found in pure ethanol. Finally,
757 carotenoids were primarily extracted by 100% ethanol, but their content decreased with
758 the temperature, indicating the possibility of compound degradation. Optimum

759 extraction conditions for PLE and MAE were modeled to maximize each response
760 variable, all response variables, and all variables except the yield (**Table 5**). HPLC–
761 APCI–MS/MS was used to characterize the extracts obtained at optimum conditions.
762 Fucoxanthin was the most abundant compound; then diatoxanthin, other two
763 carotenoids, and one carotenoid ester were detected. Other minor peaks in the
764 chromatogram were attributed to chlorophylls, having the same absorbance
765 spectrum. The amount of fucoxanthin recovered in PLE and MAE is also presented in
766 **Table 5**. MAE optimum extracts were richer in phenols, carotenoids, and TEAC;
767 however, higher extraction yields were obtained from PLE. Regarding fucoxanthin, its
768 concentration was similar between MAE and PLE extracts, but its recovery was better
769 with PLE technology thanks to the higher extraction yield (Gilbert-López et al., 2017).
770

771

Optimum modeled extraction conditions	PLE	MAE	Recovered fucoxanthin [mg g^{-1} algae]
Yield maximization	170 °C; 40% EtOH	170 °C; pure water; 20 min	-
TPC maximization	50 °C; 100% EtOH	30 °C; 100% EtOH; 2 min	7.73 (PLE)
TEAC maximization	50 °C; 100% EtOH	170 °C; 100% EtOH; 2 min	
Carotenoids maximization	170 °C; 100% EtOH	30 °C; 100% EtOH; 2 min	-
Yield, TPC, TEAC, and carotenoids maximization	170 °C; 97% EtOH	170 °C; 100% EtOH; 5.8 min	5.81 (PLE), 2.97 (MAE)
TPC, TEAC and carotenoids maximization	50 °C; 100% EtOH	30 °C; 100% EtOH; 2min	4.59 (MAE)

772

773 **Table 5.** Modeled optimum conditions for extraction of valuable compounds from *P.*

774 *tricornutum* using PLE and MAE.

775

776 Tommasi et al. (2017) also explored the lipid extraction from *P. tricornutum* (furnished
777 by Micoperi Blue Growth) by using dimethyl carbonate (DMC) solvent extraction (a
778 nonvolatile, cheap, non-corrosive, non-toxic, and eco-friendly solvent) and supercritical
779 CO_2 ($scCO_2$). Microwaves (MWs) and deep eutectic solvents (DESs) and their
780 combination were used as pretreatments for both extractions and their performances
781 were evaluated. The authors tested the application of different DESs obtained by
782 choline chloride and diverse hydrogen donors, concluding that DESs obtained by ChCl
783 and carboxylic acids was the best solvent among the tested ones, as higher selectivity
784 and an enhancement of total fatty acid (TFA) extraction performances of DMC were
785 determined. Instead, the MW process alone did not enhance DMC extraction capacity,
786 which remained scarcely effective or selective. The combination of DESs and MW
787 pretreatments and the subsequent DMC extraction resulted in a TFA yield and fatty acid
788 profile similar to those obtained by the conventional Bligh and Dyer procedure, together
789 with a much-improved selectivity (88% against 35%). The combination DES-MW
790 remarkably enhanced the extraction efficiency of scCO2, improving the TFA yield by
791 20-fold and obtaining very purified extracts. Despite DES-scCO2 extracting lower
792 quantities of total fatty acids than DES−MW-scCO2, it resulted in the highest content of
793 EPA (35%). Neither DES nor DES−MW pretreatments were found to degrade PUFAs
794 and EPA, which hence can be effectively extracted employing DMC and scCO2
795 procedures (Tommasi et al., 2017). No other extraction technologies have been
796 proposed and tested for *P. tricornutum* so far, except for some studies concerning the
797 combined production of diverse value-added compounds in a biorefinery approach that
798 will be discussed in the next section. Hence, other, especially environmentally friendly
799 techniques should be assessed on this interesting diatom both to identify the best

extraction conditions leading to the highest yields and to determine what is extracted and what remains in the residual if it is undamaged, thus exploring the possibility of a cascade extraction and purification of algae biomass.

3.1 Biorefinery approaches

Currently, at a commercial scale, just a single compound (e.g., astaxanthin, ß-carotene) is produced from microalgae sources, while other conceivably fractions such as proteins and carbohydrates, are disposed of. Instead, to enhance the economic feasibility of bioactive compounds production from microalgae, all biomass fractions should be valorised, leading to a multi-product biorefinery (Bhattacharya and Goswami, 2020; Branco-Vieira et al., 2020). A microalgae-based biorefinery would then rely on an industrial chain producing microalgal biomass under optimal conditions and, subsequently, a facility generating a broad range of products, such as chemicals, food additives, health-enhancing compounds, and biofuels, exactly as occurs for petroleum-based processes (Gilbert-López et al., 2015). Some studies developed and tested cascade extractions on *P. tricornutum* to obtain multiple compounds production in a perspective of biorefinery. For example, a multi-step aqueous and non-aqueous extraction was developed for *P. tricornutum* biomass provided by Algosource Saint-Nazaire, as follows: high voltage electrical discharges (HVED: 1-8 ms; 40 kV cm^{-1}) or high-pressure homogenization (HPH: 10 passes; 1200 bar) (first step); aqueous extraction to obtain carbohydrates, proteins, and water-soluble pigments (second step); liposoluble pigments extraction by 95% ethanol (third step); and lipids extraction by chloroform and methanol (fourth step). Characterizations of proteins, carbohydrates, ionic compounds, and hydro-soluble pigments were conducted to test the extraction performances of the two pre-treatments employed. The authors showed how HVED

performed better selective extraction of hydro-soluble compounds. However, the efficiency of HPH treatment in disrupting microalgal cells and extracting hydro-soluble compounds (carbohydrates and proteins) was higher; while the non-aqueous extraction (third and fourth steps) of pigments and lipids was more efficient when HVED was used. Overall, the pre-treatments allowed to improve the amounts of components of interest in the extracts, compared to the untreated samples (Zhang et al., 2020). **Figure 2a** shows another stepwise extraction procedure to produce multiple-valued compounds from the same biomass of *P. tricornutum*, used as lyophilized biomass from Phytobloom Necton. A crude extract was first obtained using methanol (20% v/v); successively, chloroform and methanol (2:1 v/v) were adopted to obtain total lipids from the remaining biomass, and finally, the "leftover" material, was subjected to anaerobic digestion to assess its Biochemical Methane Potential (BMP). The crude extract obtained from the first step was further separated into a hydrophilic fraction and a lipophilic one by adding 0.05 volumes of chloroform. Obtained fractions from the extraction protocol were then characterized using NMR analysis, bioactivity test, and fatty acid profile analysis. The lipid content of the residue from step 2 was 17.09% ± 1.50%. Final exhausted biomass provided an Organic Fraction content of 88.07 ± 0.50% and led to 164.8 ± 10.3 ml g^{-1} of organic fraction as methane yield (Savio et al., 2020). Another study proposed a stepwise extraction process on *P. tricornutum* to obtain EPA, chrysolaminarin, and fucoxanthin in a biorefinery concept, utilizing different solvent solutions **(Figure 2b)**. The algal powder was first subjected to a Microwave-Assisted Extraction with ethanol; then both extract and residue were treated with hexane and resulted in three fractions: hydroalcoholic phase, which was further purified to obtain fucoxanthin, hexane phase, which gave a concentrate in EPA after few other steps, and

a residue, from which chrysolaminarin was separated. The yields obtained were 34.03 ± 0.72%, 23.00 ± 0.29%, and 43.54 ± 0.91% DW, respectively. Moreover, the use of ethanol and MW treatments of 1 min resulted in the highest fucoxanthin yield (Zhang et al., 2018). Although these works are the first reports on the comprehensive utilization of *P. tricornutum* biomass, the use of toxic solvents was still selected. Moreover, as depicted in **Figure 2b**, the developed step-wise extraction is composed of numerous steps, which could be hardly scaled up at the industrial level. Hence, it should be further explored the possibility of designing a biorefinery based on *P. tricornutum* biomass making ideal use of exclusively green extraction technologies and safe solvents.

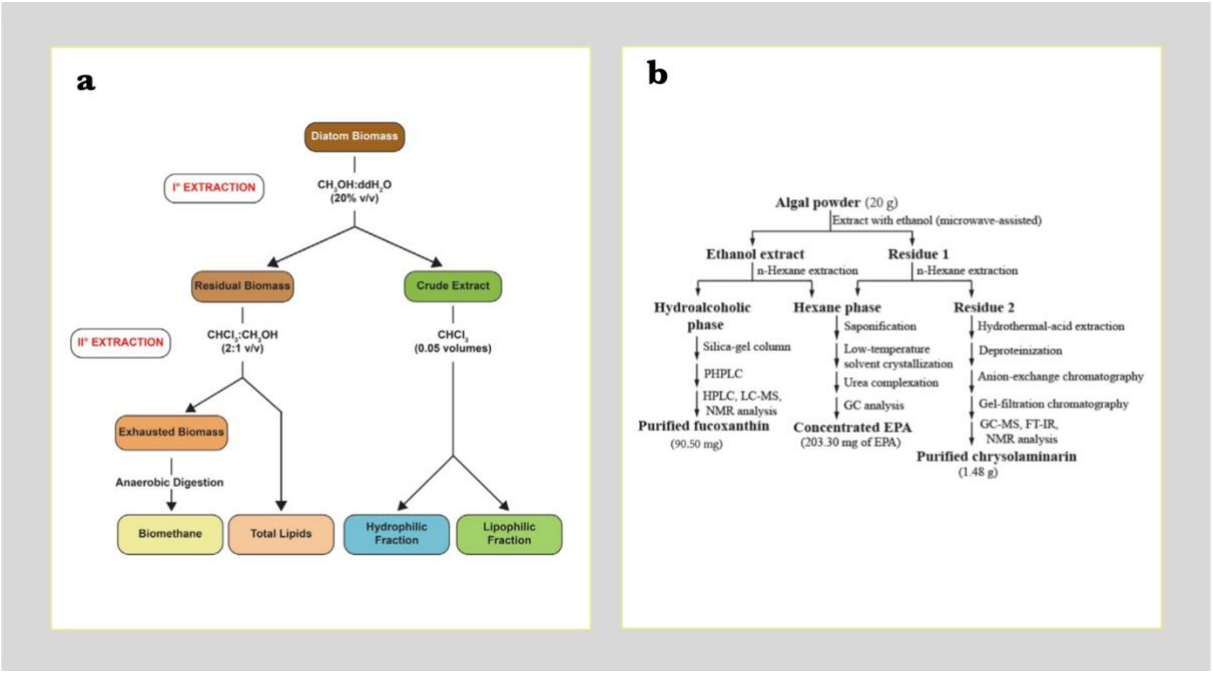

Figure 2. Step-wise extraction of value-added compounds from *P. tricornutum* biomass in a biorefinery perspective. **a)** (Savio et al., 2020) **b)** (Zhang et al., 2018)

4. Conclusions

As illustrated, *Phaeodactylum tricornutum* shows great potential in the microalgae sector to produce valuable compounds. Glycerol was confirmed as the best organic source for growing this diatom mixotrophically, enhancing both biomass concentration and growth rate. Beyond EPA, fucoxanthin, and chrysolaminarin, other valuable compounds worth to be studied could be present in extraction biomass residuals. Therefore, more effort should be addressed to the study of green extraction methods in a biorefinery concept, also exploring the possibility of using wet extraction methods thus saving the energy required for the drying step. Finally, techno-economic analysis and Life Cycle Assessment could be used to assess the effective potential of a microalgae-biorefinery.

5. Acknowledgments

This research did not receive any specific grant from funding agencies in the public, commercial, or not-for-profit sectors.

6. References

1. Araújo, R., Vázquez Calderón, F., Sánchez López, J., Azevedo, I.C., Bruhn, A., Fluch, S., Garcia Tasende, M., Ghaderiardakani, F., Ilmjärv, T., Laurans, M., Mac Monagail, M., Mangini, S., Peteiro, C., Rebours, C., Stefansson, T., Ullmann, J., 2021. Current Status of the Algae Production Industry in Europe: An Emerging Sector of the Blue Bioeconomy. Front. Mar. Sci. 7, 1247. https://doi.org/10.3389/FMARS.2020.626389/BIBTEX
2. Bhattacharya, M., Goswami, S., 2020. Microalgae – A green multi-product biorefinery for future industrial prospects. Biocatal. Agric. Biotechnol. 25, 101580. https://doi.org/10.1016/J.BCAB.2020.101580

3. Branco-Vieira, M., Martin, S.S., Agurto, C., Freitas, M.A.V., Mata, T.M., Martins, A.A., Caetano, N., 2018. Phaeodactylum tricornutum derived biosilica purification for energy applications. Energy Procedia 153, 279–283. https://doi.org/10.1016/J.EGYPRO.2018.10.020
4. Branco-Vieira, M., San Martin, S., Agurto, C., Freitas, M.A.V., Martins, A.A., Mata, T.M., Caetano, N.S., 2020. Biotechnological potential of Phaeodactylum tricornutum for biorefinery processes. Fuel 268, 117357. https://doi.org/10.1016/J.FUEL.2020.117357
5. Butler, T., Kapoore, R.V., Vaidyanathan, S., 2020. Phaeodactylum tricornutum: A Diatom Cell Factory. Trends Biotechnol. 38, 606–622. https://doi.org/10.1016/J.TIBTECH.2019.12.023
6. Butler, T.O., Padmaperuma, G., Lizzul, A.M., McDonald, J., Vaidyanathan, S., 2022. Towards a Phaeodactylum tricornutum biorefinery in an outdoor UK environment. Bioresour. Technol. 344, 126320. https://doi.org/10.1016/j.biortech.2021.126320
7. Caballero, M.A., Jallet, D., Shi, L., Rithner, C., Zhang, Y., Peers, G., 2016. Quantification of chrysolaminarin from the model diatom Phaeodactylum tricornutum. Algal Res. 20, 180–188. https://doi.org/10.1016/j.algal.2016.10.008
8. Cerón-García, M.C., Fernández-Sevilla, J.M., Sánchez-Mirón, A., García-Camacho, F., Contreras-Gómez, A., Molina-Grima, E., 2013. Mixotrophic growth of Phaeodactylum tricornutum on fructose and glycerol in fed-batch and semi-continuous modes. Bioresour. Technol. 147, 569–576. https://doi.org/10.1016/j.biortech.2013.08.092
9. Cerón-García, M.C., Fernández Sevilla, J.M., Acién Fernández, F.G., Molina

909 Grima, E., García Camacho, F., 2000. Mixotrophic growth of Phaeodactylum
910 tricornutum on glycerol: Growth rate and fatty acid profile. J. Appl. Phycol. 12,
911 239–248. https://doi.org/10.1023/a:1008123000002
912 10. Cerón-García, M.C., Sánchez Mirón, A., Fernández Sevilla, J.M., Molina
913 Grima, E., García Camacho, F., 2005. Mixotrophic growth of the microalga
914 Phaeodactylum tricornutum: Influence of different nitrogen and organic carbon
915 sources on productivity and biomass composition. Process Biochem. 40, 297–
916 305. https://doi.org/10.1016/j.procbio.2004.01.016
917 11. Chauton, M.S., Olsen, Y., Vadstein, O., 2013. Biomass production from the
918 microalga Phaeodactylum tricornutum: Nutrient stress and chemical
919 composition in exponential fed-batch cultures. Biomass and Bioenergy 58, 87–
920 94. https://doi.org/10.1016/j.biombioe.2013.10.004
921 12. Enzing, C., Ploeg, M., Barbosa, M., Sijtsma, L., 2014. Microalgae-based
922 products for the food and feed sector: an outlook for Europe, JRC Scientific and
923 policy reports. https://doi.org/10.2791/3339
924 13. Eppink, M.H.M., Ventura, S.P.M., Coutinho, J.A.P., Wijffels, R.H., 2021.
925 Multiproduct Microalgae Biorefineries Mediated by Ionic Liquids. Trends
926 Biotechnol. https://doi.org/10.1016/J.TIBTECH.2021.02.009
927 14. Fernández Sevilla, J.M., Cerón García, M.C., Sánchez Mirón, A., Belarbi, E.H.,
928 García Camacho, F., Molina Grima, E., 2004. Pilot-Plant-Scale Outdoor
929 Mixotrophic Cultures of Phaeodactylum tricornutum Using Glycerol in Vertical
930 Bubble Column and Airlift Photobioreactors: Studies in Fed-Batch Mode.
931 Biotechnol. Prog. 20, 728–736. https://doi.org/10.1021/BP034344F
932 15. Francius, G., Tesson, B., Dague, E., Martin-Jézéquel, V., Dufrêne, Y.F., 2008.

933 Nanostructure and nanomechanics of live Phaeodactylum tricornutum
934 morphotypes. Environ. Microbiol. 10, 1344–1356.
935 https://doi.org/10.1111/J.1462-2920.2007.01551.X
936 16. Gallego, R., Montero, L., Cifuentes, A., Ibáñez, E., Herrero, M., 2018. Green
937 Extraction of Bioactive Compounds from Microalgae. J. Anal. Test. 2018 22 2,
938 109–123. https://doi.org/10.1007/S41664-018-0061-9
939 17. Gao, B., Chen, A., Zhang, W., Li, A., Zhang, C., 2017. Co-production of lipids,
940 eicosapentaenoic acid, fucoxanthin, and chrysolaminarin by Phaeodactylum
941 tricornutum cultured in a flat-plate photobioreactor under varying nitrogen
942 conditions. J. Ocean Univ. China 2017 165 16, 916–924.
943 https://doi.org/10.1007/S11802-017-3174-2
944 18. Gilbert-López, B., Barranco, A., Herrero, M., Cifuentes, A., Ibáñez, E., 2017.
945 Development of new green processes for the recovery of bioactives from
946 Phaeodactylum tricornutum. Food Res. Int. 99, 1056–1065.
947 https://doi.org/10.1016/j.foodres.2016.04.022
948 19. Gilbert-López, B., Mendiola, J.A., Fontecha, J., Broek, L.A.M. van den, Sijtsma,
949 L., Cifuentes, A., Herrero, M., Ibáñez, E., 2015. Downstream processing of
950 Isochrysis galbana: a step towards microalgal biorefinery. Green Chem. 17,
951 4599–4609. https://doi.org/10.1039/C5GC01256B
952 20. Gómez-Loredo, A., Benavides, J., Rito-Palomares, M., 2016. Growth kinetics
953 and fucoxanthin production of Phaeodactylum tricornutum and Isochrysis
954 galbana cultures at different light and agitation conditions. J. Appl. Phycol. 28,
955 849–860. https://doi.org/10.1007/s10811-015-0635-0
956 21. Günerken, E., D'Hondt, E., Eppink, M.H.M., Garcia-Gonzalez, L., Elst, K.,

957 Wijffels, R.H., 2015. Cell disruption for microalgae biorefineries. Biotechnol.
958 Adv. 33, 243–260. https://doi.org/10.1016/J.BIOTECHADV.2015.01.008
959 22. He, L., Han, X., Yu, Z., 2014. A Rare Phaeodactylum tricornutum Cruciform
960 Morphotype: Culture Conditions, Transformation and Unique Fatty Acid
961 Characteristics. PLoS One 9, e93922.
962 https://doi.org/10.1371/JOURNAL.PONE.0093922
963 23. Hockin, N.L., Mock, T., Mulholland, F., Kopriva, S., Malin, G., 2012. The
964 Response of Diatom Central Carbon Metabolism to Nitrogen Starvation Is
965 Different from That of Green Algae and Higher Plants. Plant Physiol. 158, 299–
966 312. https://doi.org/10.1104/PP.111.184333
967 24. Huete-Ortega, M., Okurowska, K., Kapoore, R.V., Johnson, M.P., Gilmour,
968 D.J., Vaidyanathan, S., 2018. Effect of ammonium and high light intensity on
969 the accumulation of lipids in Nannochloropsis oceanica (CCAP 849/10) and
970 Phaeodactylum tricornutum (CCAP 1055/1). Biotechnol. Biofuels 11, 1–15.
971 https://doi.org/10.1186/s13068-018-1061-8
972 25. Jallet, D., Caballero, M.A., Gallina, A.A., Youngblood, M., Peers, G., 2016.
973 Photosynthetic physiology and biomass partitioning in the model diatom
974 Phaeodactylum tricornutum grown in a sinusoidal light regime. Algal Res. 18,
975 51–60. https://doi.org/10.1016/J.ALGAL.2016.05.014
976 26. Kadalag, N.L., Pawar, P.R., Prakash, G., 2021. Co-cultivation of Phaeodactylum
977 tricornutum and Aurantiochytrium limacinum for polyunsaturated omega-3 fatty
978 acids production. Bioresour. Technol. 346, 126544.
979 https://doi.org/10.1016/j.biortech.2021.126544
980 27. Kooistra, W.H.C.F., Gersonde, R., Medlin, L.K., Mann, D.G., 2007. The Origin

and Evolution of the Diatoms: Their Adaptation to a Planktonic Existence. Evol. Prim. Prod. Sea 207–249. https://doi.org/10.1016/B978-012370518-1/50012-6

28. Kroth, P.G., Chiovitti, A., Gruber, A., Martin-Jezeque, V., Mock, T., Parker, M.S., Stanley, M.S., Kaplan, A., Caron, L., Weber, T., Maheswari, U., Armbrust, E.V., Bowler, C., 2008. A model for carbohydrate metabolism in the diatom Phaeodactylum tricornutum deduced from comparative whole genome analysis. PLoS One 3. https://doi.org/10.1371/journal.pone.0001426
29. Kuczynska, P., Jemiola-Rzeminska, M., Nowicka, B., Jakubowska, A., Strzalka, W., Burda, K., Strzalka, K., 2020. The xanthophyll cycle in diatom Phaeodactylum tricornutum in response to light stress. Plant Physiol. Biochem. 152, 125–137. https://doi.org/10.1016/j.plaphy.2020.04.043
30. Malviya, S., Scalco, E., Audic, S., Vincent, F., Veluchamy, A., Poulain, J., Wincker, P., Iudicone, D., De Vargas, C., Bittner, L., Zingone, A., Bowler, C., 2016. Insights into global diatom distribution and diversity in the world's ocean. Proc. Natl. Acad. Sci. U. S. A. 113, E1516–E1525. https://doi.org/10.1073/PNAS.1509523113/-/DCSUPPLEMENTAL
31. McClure, D.D., Luiz, A., Gerber, B., Barton, G.W., Kavanagh, J.M., 2018. An investigation into the effect of culture conditions on fucoxanthin production using the marine microalgae Phaeodactylum tricornutum. Algal Res. 29, 41–48. https://doi.org/10.1016/j.algal.2017.11.015
32. McDowell, D., Dick, J.T., Eagling, L., Julius, M., Sheldrake, G.N., Theodoridou, K., Walsh, P.J., 2020. Recycling nutrients from anaerobic digestates for the cultivation of Phaeodactylum tricornutum: A feasibility study. Algal Res. 48, 101893. https://doi.org/10.1016/j.algal.2020.101893

33. Murchie, E.H., Lawson, T., 2013. Chlorophyll fluorescence analysis: A guide to good practice and understanding some new applications. J. Exp. Bot. 64, 3983–3998. https://doi.org/10.1093/jxb/ert208

34. Not, F., Siano, R., Kooistra, W.H.C.F., Simon, N., Vaulot, D., Probert, I., 2012. Diversity and Ecology of Eukaryotic Marine Phytoplankton, Advances in Botanical Research. Elsevier. https://doi.org/10.1016/B978-0-12-391499-6.00001-3

35. Penhaul Smith, J.K., Hughes, A.D., McEvoy, L., Day, J.G., 2020. Tailoring of the biochemical profiles of microalgae by employing mixotrophic cultivation. Bioresour. Technol. Reports 9, 100321. https://doi.org/10.1016/j.biteb.2019.100321

36. Pereira, H., Sá, M., Maia, I., Rodrigues, A., Teles, I., Wijffels, R.H., Navalho, J., Barbosa, M., 2021. Fucoxanthin production from Tisochrysis lutea and Phaeodactylum tricornutum at industrial scale. Algal Res. 56, 102322. https://doi.org/10.1016/J.ALGAL.2021.102322

37. Qiao, H., Cong, C., Sun, C., Li, B., Wang, J., Zhang, L., 2016. Effect of culture conditions on growth, fatty acid composition and DHA/EPA ratio of Phaeodactylum tricornutum. Aquaculture 452, 311–317. https://doi.org/10.1016/j.aquaculture.2015.11.011

38. Rodolfi, L., Biondi, N., Guccione, A., Bassi, N., D'Ottavio, M., Arganaraz, G., Tredici, M.R., 2017. Oil and eicosapentaenoic acid production by the diatom Phaeodactylum tricornutum cultivated outdoors in Green Wall Panel (GWP®) reactors. Biotechnol. Bioeng. 114, 2204–2210. https://doi.org/10.1002/BIT.26353

1029 39. Savio, S., Farrotti, S., Paris, D., Arnaìz, E., Díaz, I., Bolado, S., Muñoz, R.,
1030 Rodolfo, C., Congestri, R., 2020. Value-added co-products from biomass of the
1031 diatoms Staurosirella pinnata and Phaeodactylum tricornutum. Algal Res. 47,
1032 101830. https://doi.org/10.1016/J.ALGAL.2020.101830
1033 40. Silva Benavides, A.M., Torzillo, G., Kopecký, J., Masojídek, J., 2013.
1034 Productivity and biochemical composition of Phaeodactylum tricornutum
1035 (Bacillariophyceae) cultures grown outdoors in tubular photobioreactors and
1036 open ponds. Biomass and Bioenergy 54, 115–122.
1037 https://doi.org/10.1016/j.biombioe.2013.03.016
1038 41. Simonazzi, M., Pezzolesi, L., Guerrini, F., Vanucci, S., Samorì, C., Pistocchi,
1039 R., 2019. Use of waste carbon dioxide and pre-treated liquid digestate from
1040 biogas process for Phaeodactylum tricornutum cultivation in photobioreactors
1041 and open ponds. Bioresour. Technol. 292, 121921.
1042 https://doi.org/10.1016/J.BIORTECH.2019.121921
1043 42. Song, M., Pei, H., Hu, W., Han, F., Ji, Y., Ma, G., Han, L., 2014. Growth and
1044 lipid accumulation properties of microalgal Phaeodactylum tricornutum under
1045 different gas liquid ratios. Bioresour. Technol. 165, 31–37.
1046 https://doi.org/10.1016/j.biortech.2014.03.070
1047 43. Song, Z., Lye, G.J., Parker, B.M., 2020. Morphological and biochemical
1048 changes in Phaeodactylum tricornutum triggered by culture media: Implications
1049 for industrial exploitation. Algal Res. 47, 101822.
1050 https://doi.org/10.1016/J.ALGAL.2020.101822
1051 44. Su, M., D'Imporzano, G., Veronesi, D., Afric, S., Adani, F., 2020.
1052 Phaeodactylum tricornutum cultivation under mixotrophic conditions with

glycerol supplied with ultrafiltered digestate: A simple biorefinery approach recovering C and N. J. Biotechnol. 323, 73–81. https://doi.org/10.1016/j.jbiotec.2020.07.018

45. Sun, J., Zhou, C., Cheng, P., Zhu, J., Hou, Y., Li, Y., Zhang, J., Yan, X., 2022. A simple and efficient strategy for fucoxanthin extraction from the microalga Phaeodactylum tricornutum. Algal Res. 61, 102610. https://doi.org/10.1016/j.algal.2021.102610

46. Tesson, B., Gaillard, C., Martin-Jézéquel, V., 2009. Insights into the polymorphism of the diatom Phaeodactylum tricornutum Bohlin. Bot. Mar. 52, 104–116. https://doi.org/10.1515/BOT.2009.012

47. Tommasi, E., Cravotto, G., Galletti, P., Grillo, G., Mazzotti, M., Sacchetti, G., Samorì, C., Tabasso, S., Tacchini, M., Tagliavini, E., 2017. Enhanced and Selective Lipid Extraction from the Microalga P. tricornutum by Dimethyl Carbonate and Supercritical CO2 Using Deep Eutectic Solvents and Microwaves as Pretreatment. ACS Sustain. Chem. Eng. 5, 8316–8322. https://doi.org/10.1021/ACSSUSCHEMENG.7B02074/SUPPL_FILE/SC7B02074_SI_001.PDF

48. Villanova, V., Fortunato, A.E., Singh, D., Bo, D.D., Conte, M., Obata, T., Jouhet, J., Fernie, A.R., Marechal, E., Falciatore, A., Pagliardini, J., Le Monnier, A., Poolman, M., Curien, G., Petroutsos, D., Finazzi, G., 2017. Investigating mixotrophic metabolism in the model diatom phaeodactylum tricornutum. Philos. Trans. R. Soc. B Biol. Sci. 372. https://doi.org/10.1098/rstb.2016.0404

49. Villanova, V., Singh, D., Pagliardini, J., Fell, D., Le Monnier, A., Finazzi, G., Poolman, M., 2021. Boosting Biomass Quantity and Quality by Improved

Mixotrophic Culture of the Diatom Phaeodactylum tricornutum. Front. Plant Sci. 0, 411. https://doi.org/10.3389/FPLS.2021.642199

50. Wang, S., Said, I.H., Thorstenson, C., Thomsen, C., Ullrich, M.S., Kuhnert, N., Thomsen, L., 2018. Pilot-scale production of antibacterial substances by the marine diatom Phaeodactylum tricornutum Bohlin. Algal Res. 32, 113–120. https://doi.org/10.1016/j.algal.2018.03.014
51. Wang, X.W., Huang, L., Ji, P.Y., Chen, C.P., Li, X.S., Gao, Y.H., Liang, J.R., 2019. Using a mixture of wastewater and seawater as the growth medium for wastewater treatment and lipid production by the marine diatom Phaeodactylum tricornutum. Bioresour. Technol. 289, 121681. https://doi.org/10.1016/j.biortech.2019.121681
52. Wang, Z., Mou, J., Qin, Z., He, Y., Sun, Z., Wang, X., Sze Ki Lin, C., 2021. An auxin-like supermolecule to simultaneously enhance growth and cumulative eicosapentaenoic acid production in Phaeodactylum tricornutum. Bioresour. Technol. 345, 126564. https://doi.org/10.1016/j.biortech.2021.126564
53. Yodsuwan, N., Sawayama, S., Sirisansaneeyakul, S., 2017. Effect of nitrogen concentration on growth, lipid production and fatty acid profiles of the marine diatom Phaeodactylum tricornutum. Agric. Nat. Resour. 51, 190–197. https://doi.org/10.1016/j.anres.2017.02.004
54. Zhang, R., Lebovka, N., Marchal, L., Vorobiev, E., Grimi, N., 2020. Multistage aqueous and non-aqueous extraction of bio-molecules from microalga Phaeodactylum tricornutum. Innov. Food Sci. Emerg. Technol. 62, 102367. https://doi.org/10.1016/J.IFSET.2020.102367
55. Zhang, W., Wang, F., Gao, B., Huang, L., Zhang, C., 2018. An integrated

biorefinery process: Stepwise extraction of fucoxanthin, eicosapentaenoic acid and chrysolaminarin from the same Phaeodactylum tricornutum biomass. Algal Res. 32, 193–200. https://doi.org/10.1016/j.algal.2018.04.002

56. Zhou, X., Jin, W., Tu, R., Guo, Q., Han, S. fang, Chen, C., Wang, Qing, Liu, W., Jensen, P.D., Wang, Qilin, 2019. Optimization of microwave assisted lipid extraction from microalga Scenedesmus obliquus grown on municipal wastewater. J. Clean. Prod. 221, 502–508. https://doi.org/10.1016/J.JCLEPRO.2019.02.260